

Dynamics of shear homeomorphisms of tori and the Bestvina-Handel algorithm

Tali Pinski and Bronislaw Wajnryb

ABSTRACT

Sharkovskii proved that the existence of a periodic orbit in a one-dimensional dynamical system implies existence of infinitely many periodic orbits. We obtain an analog of Sharkovskii's theorem for periodic orbits of shear homeomorphisms of the torus. This is done by obtaining a dynamical order relation on the set of simple orbits and simple pairs. We then use this order relation for a global analysis for a quantum chaotic physical system called the kicked accelerated particle.

1. INTRODUCTION

Given a dynamical system (X, f) , a key question is which periodic orbits exist for this system. Since periodic orbits are in general difficult to compute, we would like to have the means to deduce their existence without having to actually compute them.

Sharkovskii addressed the dynamics of continuous maps on the real line. He defined an order \triangleleft on the natural numbers, Sharkovskii's order, and proved that the existence of a periodic orbit of a certain period p implies the existence of an orbit of any period $q \triangleleft p$. We say the q orbit is *forced* by the p orbit. This offers the means of showing the existence of many orbits if one can find a single orbit of "large" period. For a dynamical system depending on a single parameter, if periodic orbits appear when we change the parameter, they must appear according to the Sharkovskii's order. Hence, Sharkovskii's theorem gives the global structure of the appearance of periodic orbits for one dimensional systems. Ever since the eighties there has been interest in obtaining analogs for Sharkovskii's theorem for two dimensional systems (see [3] and [12]).

A homeomorphism of a torus is said here to be of *shear type* if it is isotopic to one Dehn twist along a single closed curve. There exists a basis for the first homology for which the induced map is represented by

the matrix $\begin{pmatrix} 1 & 0 \\ 1 & 1 \end{pmatrix}$. From here on we refer to any two axes given by an homology basis that gives us the above representation as *standard axes*. Let h be a shear homeomorphism, and let x be a periodic orbit of h . We can then define the *rotation number* of x , see discussion in Section 3. Thus, a rational number in the unit interval $[0, 1]$ is associated to each orbit.

We consider orbits up to conjugation: orbits (x, f) and (y, g) are similar if there exists a diffeomorphism h of the torus T^2 which takes orbit x onto orbit y and hfh^{-1} is isotopic to g rel y . We define below a specific family of periodic orbits we call simple orbits. In this family there is a unique element up to similarity corresponding to each rotation number; hence they can be specified by their rotation numbers. We emphasize it is not true in general that an orbit of a shear homeomorphism is characterized by its rotation number.

These orbits are analyzed in Section 3. As it turns out, one simple orbit is indeed simple, and does not force enough dynamics. Hence we turn in Section 4 to analyze pairs of orbits. Two coexisting simple periodic orbits can form a simple pair and these are considered. The pairs do force some more interesting dynamics, as follows. For a pair of simple orbits of rotation numbers $\frac{q_1}{p_1}$ and $\frac{q_2}{p_2}$ to constitute a simple pair, it is necessary that the rotation numbers be Farey neighbors, i.e. $|p_2q_1 - p_1q_2| = 1$. We denote such a pair of rationales by $\frac{q_1}{p_1} \vee \frac{q_2}{p_2}$.

We now define an order relation on the set of rational numbers and pairs. Denote \mathcal{P} to be the set

$$\mathcal{P} = \{q | q \in \mathbb{Q} \cap [0, 1]\} \cup \{q \vee p | q, p \in \mathbb{Q} \cap [0, 1]\}.$$

Define the order relation on \mathcal{P} to be

$$q \vee p \succ r \Leftrightarrow r \in [q, p]$$

and

$$q \vee p \succ r \vee s \Leftrightarrow r, s \in [q, p].$$

Where we denote by $[q, p]$ the interval between q and p , regardless of their order.

Theorem 1.1. *The order relation \succ on \mathcal{P} describes the dynamical forcing of simple periodic orbits. The existence of a simple pair of periodic orbits with rotation numbers $q \vee p$ in \mathcal{P} implies the existence of all simple orbits and simple orbit pairs of rotation numbers smaller than $q \vee p$ according to this order relation.*

This is the main result of this paper and the proof is completed in Section 5. The idea of the proof is as follows. Consider the torus punctured on one or more periodic orbits of a homeomorphism h . Then h induces an action on this punctured torus, and on its (free) fundamental group. Now apply the Bestvina-Handel algorithm to this dynamical system. The idea of using the Bestvina-Handel algorithm was used by Boyland in [5] and he describes the general approach in [4]. In our case, after puncturing out a simple pair of orbits, applying the algorithm yields an isotopic homeomorphism which is pseudo-Anosov. Furthermore, the algorithm offers a Markov partition for this system, together with a symbolic representation. We use the symbolic representation to find that there are periodic orbits of each rotation number between the pair of numbers we started with. Then we directly analyze the structure of the pseudo-Anosov representative to show that all these orbits are in fact simple orbits. Furthermore any two of them corresponding to rotation numbers which are Farey neighbors form a simple pair. Finally we establish the isotopy stability of these orbits using Boyland's results in [5]. Thus, they exist for any homeomorphism for which the simple pair exists, and are forced by it.

One should compare this result with a very strong theorem of Doeff (see Theorem 4.6), where existence of two periodic orbits of different periods for a given homeomorphism h implies existence of periodic orbit of every intermediate rotation number. However nothing is said about the dynamics of h in the complement of these orbits while our theorem implies existence of periodic orbits and pairs of orbits with precisely described behavior.

This research was originally motivated by a question we were asked by Professor Shmuel Fishman: Is there a topological explanation for the structure of appearance of accelerator modes in the kicked particle system. In section 6 we give a description of the kicked particle system. This system turns out to be described precisely by a family of shear homeomorphisms of the torus. The existence of accelerator modes is equivalent to existence of periodic orbits. The global structure of this system is thus given entirely by the order relation in Theorem 1.1, while it cannot be directly computed due to the complexity of the system.

The authors would like to thank Professor Shmuel Fishman for offering valuable insights, Professor Italo Guannieri for some critical advice, and Professor Philip Boyland for many indispensable conversations.

2. PRELIMINARIES

A *fibred surface* is a compact surface F with boundary such that F is decomposed into arcs and polygons called decomposition elements. The boundaries of the arcs are contained in the boundary of the surface. The polygons form k -junctions for natural k , as in Figure 1

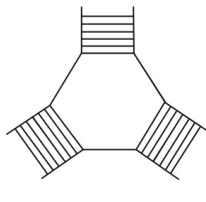


FIGURE 1. Part of a fibred surface containing a 3-junction

A fibred surface $F \subset S_0$ carries a homeomorphism f if $F \hookrightarrow S_0$ is a homotopy equivalence, f maps each decomposition element of F into a decomposition element and each junction into a junction.

A fibred surface gives rise to a graph, which is its spine and can be constructed by collapsing each decomposition element to a point. A homeomorphism carried by the fibred surface then induces a map on this graph. The converse is also true: a given action on a graph which is a spine of a punctured surface S_0 determines an action on S_0 up to isotopy. We therefore specify the periodic orbits we analyze in terms of the action on a graph which is a deformation retract of the surface after puncturing out the orbit.

For a set of points $\{x_1, \dots, x_N\}$ belonging to one or more periodic orbits for a homeomorphism f of a surface S we can look at the action on their complement $S_0 = S \setminus \{x_1, \dots, x_N\}$. Choose any graph G which is a deformation retract of the punctured surface S_0 . Let \tilde{f} be a homeomorphism isotopic to f such that \tilde{f} is fixed outside some regular neighborhood S_1 of G . Then, endowing this neighborhood with a fibred surface structure in the natural way, we may isotop f further to be carried by the fibred surface. The spine will exactly match the graph G we chose, with an induced action.

The Thurston-Nielsen classification theorem, see [7], states that any homeomorphism f on a compact connected oriented surface of negative Euler characteristic is isotopic to a homeomorphism \tilde{f} which is

- (1) pseudo Anosov, or
- (2) of finite order, or

(3) reducible.

where a homeomorphism ϕ is called *of finite order* if there exists a natural number n such that $\phi^n = id$. A homeomorphism ϕ is called *pseudo-Anosov* if there exists a real number $\lambda > 0$ and a pair of transverse measured foliations (\mathcal{F}^u, μ^u) and (\mathcal{F}^s, μ^s) with $\phi(\mathcal{F}^u, \mu^u) = (\mathcal{F}^u, \lambda\mu^u)$ and $\phi(\mathcal{F}^s, \mu^s) = (\mathcal{F}^s, \frac{1}{\lambda}\mu^s)$. A homeomorphism ϕ on a surface M is called *reducible* if there exists a collection of pairwise disjoint simple closed curves $\Gamma = \{\Gamma_1, \dots, \Gamma_k\}$ in $int(M)$ such that $\phi(\Gamma) = \Gamma$ and each component of $M \setminus \Gamma$ has a negative Euler characteristic. The representative \tilde{f} in the isotopy class of f which is of one of the three forms above is called the Thurston-Nielsen canonical form of f .

The surface S_1 in our case is a punctured torus and hence always has a negative Euler characteristic. It has a fibered surface structure and carries f . This allows us to apply the Bestvina-Handel algorithm (see [2]), which is an algorithm determining the type of f according to the classification above. The algorithm specifies a finite number of steps which we apply to the graph G we constructed as the spine of S_0 , altering G together with the induced action on it, but without changing the isotopy class of f on S_0 . When the algorithm stops, it gives a new homeomorphism \tilde{f} which is the Thurston Nielsen canonical form of f . If the homeomorphism \tilde{f} we get is a pseudo Anosov homeomorphism, the fibered surface structure given at the end of the algorithm gives a canonical way of endowing the surface S_1 with a rectangle decomposition $\{R_1, \dots, R_N\}$. The decomposition is a Markov partition for the homeomorphism \tilde{f} , meaning these rectangles are mapped nicely to each other.

From the action of \tilde{f} on the Markov partition we get a symbolic representation for the dynamical system (S_1, \tilde{f}) in the following way. Let Σ be the subset of the full N -shift (the set of bi-infinite series on N symbols), where N is the number of rectangles in the decomposition, defined by

$$\Sigma = \{s = (\dots, s_n, s_{n+1}, \dots) : R_{s_n} \cap \tilde{f}^{-1}R_{s_{n+1}} \neq \emptyset\}$$

On Σ we naturally define a dynamical system with the operator of the right shift denoted by σ , and (Σ, σ) is called the subshift corresponding to the dynamical system. Σ can be completely described by stating which transitions $k \rightarrow m$ for $k, m \in \{1, \dots, N\}$ are *allowed* (i.e., for which k, m , $\tilde{f}^{-1}R_m \cap R_k \neq \emptyset$). This list of allowed transitions are called *transition rules*. See [1] for the definitions and for a proof that in this case we can define a map $\pi : \Sigma \rightarrow S_0$ by

$$\pi : s \mapsto \bigcap_{n=0}^{\infty} \overline{\tilde{f}^n R_{s_{-n}} \cap \dots \cap \tilde{f}^{-n} R_{s_n}}$$

which satisfies the following properties:

- $\pi\sigma = \tilde{f}\pi$,
- π is continuous,
- π is onto.

We take here the set of sequences with the Tichonoff topology. A periodic point in the symbolic dynamical system now corresponds to a periodic point on our system of the punctured surface (as $\pi\sigma = \tilde{f}\pi$). But a periodic point in the symbolic shift is simply a periodic allowed sequence and so periodic orbits can be easily found.

Boyland's results in [5] can be now used to determine whether these new orbits are stable under isotopy. For this we have to define two types of equivalence classes for periodic orbits. We first give definitions for equivalence of periodic points. Let x_0 and y_0 be two periodic points for a homeomorphism f of a surface S with the same period p .

- x_0 and y_0 are *periodic Nielsen equivalent* if there is an arc $\gamma : [0, 1] \rightarrow M$ with $\gamma(0) = x$, $\gamma(1) = y$ and $f^p(\gamma)$ homotopic to γ with fixed endpoints.
- x and y are *abelian Nielsen equivalent* if there exists an arc γ as above and the loop $\gamma \cdot (f^n(\gamma))^{-1}$ represents the zero class in $\text{coker}(f_* - id) := H_1(M; \mathbb{Z}) / \text{Im}(f_* - id)$

Two periodic orbits x and y are called *periodic (resp. abelian) Nielsen equivalent* if there is a point from x which is periodic (abelian) Nielsen equivalent to a point from y .

An equivalence class of each of these relations is called a *periodic (abelian) Nielsen type*.

A periodic point x_0 of period p for homeomorphism f_0 is called *persistent* if for each given homomorphism f_1 with $f_t : f_0 \simeq f_1$ there is a periodic point x_1 of period p for f_1 which corresponds to x_0 under the isotopy. This means that there is an arc $\gamma : [0, 1] \rightarrow T^2$ with $\gamma(0) = x_0$, $\gamma(1) = x_1$ and the curve $f_t^p(\gamma(t))$ is homotopic to $\gamma(t)$ with fixed endpoints.

This is exactly the subject of theorem 2.4 on page 20 of [5] by Boyland. The theorem states that each orientation preserving homeomorphism of an orientable compact surface is isotopic to a condensed homeomorphism. For the condensed representative, each nonempty periodic Nielsen class of periodic orbits is persistent, and contains exactly one element.

Thus, a condensed homeomorphism is a representative of the isotopy class which is in this sense the simplest. The condensed representative is a refinement of the Thurston Nielsen canonical form. In the cases for which we use the theorem here, the homeomorphism is pseudo-Anosov.

In this case the condensed representative is effectively identical to the Thurston Nielsen canonical form, and so we need not be concerned here with the details of the construction.

3. SIMPLE ORBITS

Definition 3.1. We call a periodic orbit x for a shear homeomorphism f on the two-torus a *simple orbit* if the following hold.

- (1) There can be found a graph $G \in T^2 \setminus x$ as on Figure 2 such that $T^2 \setminus G$ is a set of topological rectangles, each containing exactly one periodic point from x .

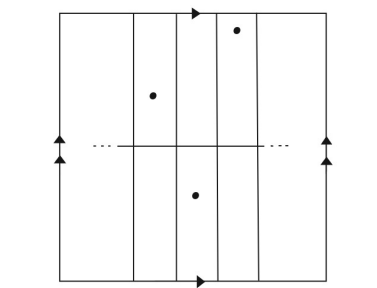


FIGURE 2. A standard graph for a simple orbit

- (2) There exists a homeomorphism \tilde{f} of $T^2 \setminus x$ isotopic to f rel x so that a neighborhood of G is invariant under \tilde{f} and the induced action on G is given as in Figure 3 where each vertical loop is mapped to another vertical loop of G which lies a fixed number of loops to its right. The horizontal loop is mapped to itself with one twist around one of the vertical loops.

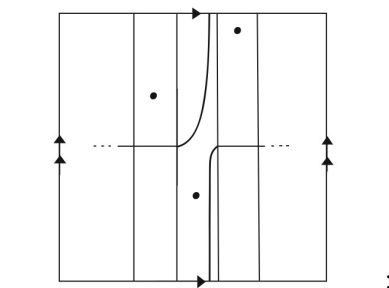


FIGURE 3. The action on a standard graph for a simple orbit

Remark. A homeomorphism h for which we are given a simple periodic orbit must be of shear type as we can deduce from the action on the homology of the non-punctured torus.

We want a simpler way to specify a simple orbit, hence we give

Definition 3.2. Let h be a shear homeomorphism, and let \hat{h} be a lift of h to the universal cover (a plane). For any periodic point x of h of period p , \hat{h}^p maps any lift \hat{x} of x the same integer number q along the horizontal axis away from \hat{x} , in a standard choice of axis (and \hat{x} is possibly mapped some integer number along the vertical axis as well). We can then define the *rotation number* of x to be $\rho(x) = \frac{q}{p} \bmod 1$. The rotation number does not depend on the lift \hat{h} of h .

Remark. In the case of a homeomorphism isotopic to a Dehn twist on a torus, which is our interest here, it can be easily shown that the abelian Nielsen type equals exactly the rotation number defined above.

There exists a simple orbit for any given rotation number r , and it is unique up to similarity. Denote the similarity class by \hat{r} . In the following we use the word vertical to describe the y axis, in a standard choice of axis for f (the direction along which the twist is made).

Lemma 3.3. *Let x be a periodic orbit for a shear-type homeomorphism f of T^2 for which there exists a family of vertical loops such that they bound a set of annuli each containing one point of the periodic orbit, and this family is invariant under a homeomorphism \tilde{f} isotopic to f rel x . Then x is a simple orbit.*

Proof. Choose a vertical loop l of the invariant family. f is orientation preserving, and so is \tilde{f} . The first loop to the right of l is therefore mapped to the first loop to the right of $\tilde{f}(l)$. Hence, the vertical loops in the invariant family are all mapped the same number of loops to the right.

Now we have to find a horizontal line with the desired image. We write the invariant family of loops as $\{l_i\}_{i=1}^p$, where $p = \text{period}(x)$, ordered along the horizontal axis. We choose another family of vertical loops $\{m_i\}_{i=1}^p$, such that m_i is contained in the annulus between l_i and l_{i+1} ($l_{p+1} = l_1$), and passes through the periodic point x_i also contained in this annulus. Choose a point $a_1 \neq x_1$ on m_1 . f can be adjusted in such a way that the new homeomorphism \tilde{f} leaves both families of vertical loops invariant, and in addition, so that a_1 be a periodic point of \tilde{f} with period p . We denote the orbit of a_1 by $\{a_i\}_{i=1}^p$ where $a_i \in m_i$ for $1 \leq i \leq p$.

Choose a line segment n_1 connecting a_1 to a_2 , so it crosses the annulus between m_1 and m_2 from side to side. We choose n_{j+1} to be the line segment $\tilde{f}^j(n_1)$ for $1 \leq j \leq p-2$. The boundary points of n_j and n_k coincide whenever they lie on the same vertical loop.

Now, we look at the horizontal loop $n = \bigcup_{j=1}^p n_j$. Each segment of n is mapped exactly to the next segment, except n_{p-1} which is mapped into the annulus between m_1 and m_2 . Since the mapping class group of an annulus is generated by a twist with respect to any loop going once around the annulus we may assume, that n_p is mapped to n_1 plus a number of twists along such a loop. On the other hand we know that $f(n)$ is homotopic to itself plus one twist in the negative direction (on the closed torus), so \tilde{f} maps n to itself plus one negative twist along this loop. By further adjustment of \tilde{f} we may assume the twist is made along l_2 . Thus the union of the vertical family $\{l_i\}$ with n chosen as above constitute a graph showing x to be a simple orbit. \square

Of course homeomorphism f is reducible with respect to a simple orbit since it contains an invariant family of loops $\{l_i\}$ and the complement of the invariant family consists of punctured annuli (which have negative Euler characteristic).

Example 1. Not every periodic orbit for a shear homeomorphism is reducible. Consider the homeomorphism h described on Figures 4 and 5. It takes the graph on Figure 4 to the graph on Figure 5, it is a shear homeomorphism, it has a periodic orbit of order 2, shown on the pictures, with rotation number $1/2$ and it is pseudo-Anosov in the complement of the orbit.

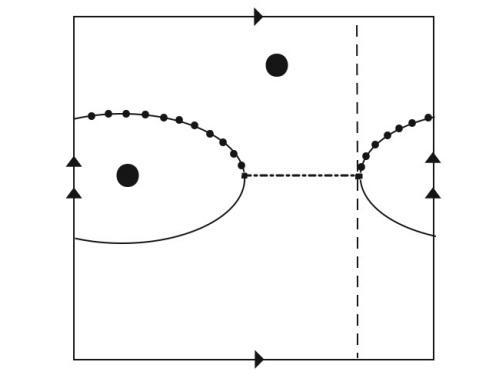


FIGURE 4.

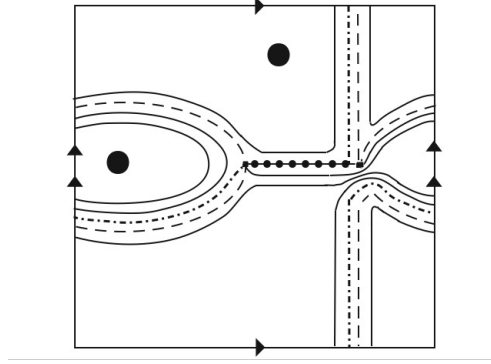


FIGURE 5.

4. SIMPLE ORBIT PAIRS

Let x and y be two coexisting simple periodic orbits, for a homeomorphism f of the two-torus T (f must be of shear type), with rotation numbers $\frac{q_1}{p_1}$ and $\frac{q_2}{p_2}$ respectively. Assume $p_1 > p_2$, i.e., y has lesser period than x .

Definition 4.1. We call the pair of orbits a simple pair if

- we can find an embedded graph on their complement as on Figure 6.

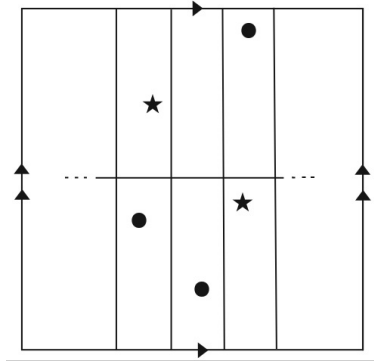


FIGURE 6.

Each component in the complement of the graph is a topological rectangle which contains exactly one point of orbit x and at most one point of orbit y .

- The homeomorphism f acts on this graph in the following way: each vertical loop except one moves to another vertical loop, there is one vertical loop denoted l such that $f(l)$ is a vertical

loop m plus a small loop around one point of the (shorter) y orbit, in a rectangle adjacent to line m on the right (as on Figure 7) or on the left, and the horizontal line is mapped to itself plus a twist in the negative direction around $f(l)$, as on Figure 7.

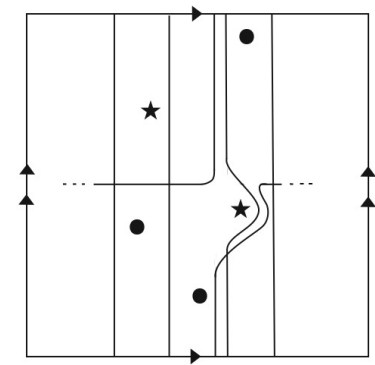


FIGURE 7.

The graph which appears in Definition 4.1 divides the torus T into p_1 rectangles. The homeomorphism f moves each vertical loop the same distance, say s rectangles, to the right except for the small additional loop for line l . Let R_0 be the rectangle adjacent to m in which the small loop in the image of the graph occurs. R_0 must contain exactly one point of each orbit. We denote these points x_0 and y_0 respectively. Under p_1 iterations of f the point x_0 runs q_1 times around the whole torus, that is $q_1 p_1$ rectangles to the right. So, $p_1 s = q_1 p_1$ and $s = q_1$.

The point y_0 is mapped to itself after p_2 iterations. Under each iteration the image of y_0 is mapped $s (= q_1)$ rectangles to the right, except the last iteration under which it is moved an additional rectangle to the right or left. Altogether it has moved $p_2 q_1 \pm 1$ rectangles. At the same time, it is mapped around the torus q_2 times, hence $q_2 p_1$ rectangles. This means $p_2 q_1 \pm 1 = q_2 p_1$. Thus for a simple pair of periodic orbits the rotation numbers $\frac{q_1}{p_1}$ and $\frac{q_2}{p_2}$ are Farey neighbors and the additional loop is on the right (as on Figure 7) if and only if $\frac{q_2}{p_2} > \frac{q_1}{p_1}$. Denote by $\hat{r} \vee \hat{s}$ the similarity class of a simple pair corresponding to a pair of Farey neighbors $r \vee s$.

Consider again the points x_0 and y_0 in the rectangle R_0 . Continue the notation to all the points of x and y by $x_i = T^i(x_0)$ and $y_i = T^i(y_0)$. We draw a small loop around each of the points of y . The union of these loops will be the peripheral subgraph P for the Bestvina-Handel algorithm, since we may assume the union of these loops to be f -invariant. Now we consider separately two cases. Case 1 will be the

case in which m is the left boundary curve of R_0 , while in case 2 it is the right boundary (in other words in the first case $\frac{q_1}{p_1} < \frac{q_2}{p_2}$ and in the second case $\frac{q_1}{p_1} > \frac{q_2}{p_2}$). Choose some point on the loop around y_0 and connect it, by a curve l_0 , to a point on the section of the horizontal line in R_0 , in case 1 from below the segment and in case 2 from above.

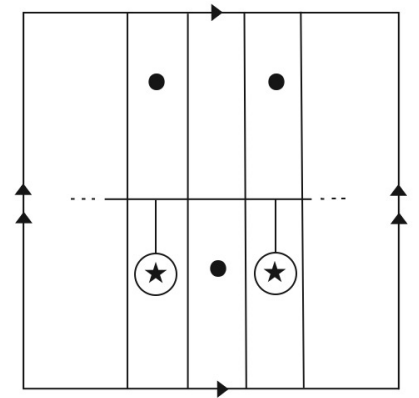


FIGURE 8.

Then $f(l_0)$ is a curve connecting the loop around y_1 and the corresponding horizontal segment. We denote it by l_1 , and do the same for each y_i . After adding the above edges to the graph case 1 is topologically as in Figure 8.

The inclusion $G \hookrightarrow S_0$ is a homotopy equivalence (where S_0 is the punctured torus). We know the action of f on all edges of G except for the curve l_{q_1-1} connecting y_{q_1-1} and the horizontal segment in the corresponding rectangle. It's image is a curve connecting the horizontal segment in the rectangle adjacent to m which is not R_0 to the loop around y_0 . This image might wind around a disk containing y_0 and x_{q_1-1} as in Figure 9

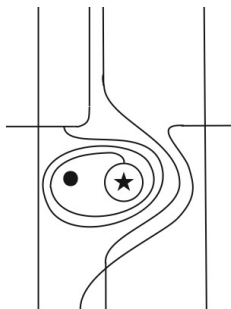


FIGURE 9.

The graph and its image for case 2 are exactly the same except that the loops are connected to the horizontal segments from above. We shall prove in Proposition 4.2 that we may assume that the image of the segment l_{q_1-1} has no winding. Hence we draw from now on the the graph images without winding. We may assume the graphs given in Figure 10 also have an invariant neighborhood by a further isotopy of f , corresponding to each of the two cases. These graphs and images are already in the form we will prove to be efficient, that is they are a terminating point for the Bestvina-Handel algorithm.

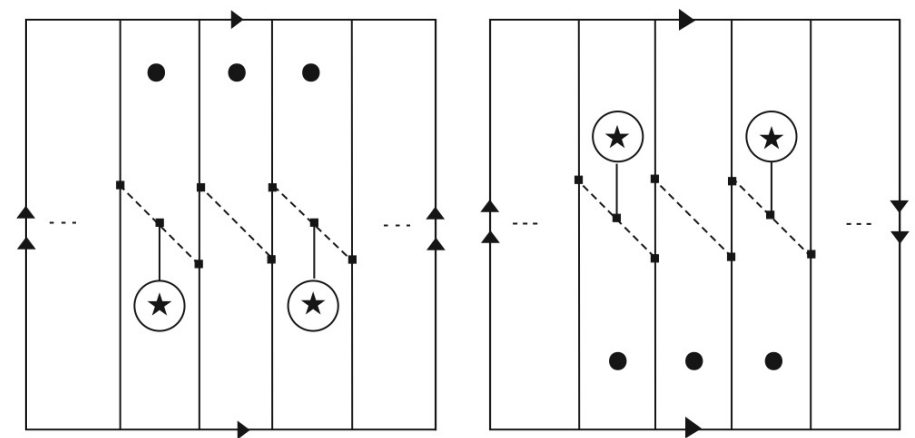


FIGURE 10. The standard graph for a simple pair, case 1 on the left and case 2 on the right.

The action of f (up to isotopy) on this graph is given by one of the actions on Figure 11, drawn in some regular neighborhood of the graph, where each vertical loop moves q_1 loops to the right.

Proposition 4.2. *Let $\{x, y\}$ be a simple pair with the graph as on Figure 8 and with windings as on Figure 9. Then there may be chosen a different invariant graph, which also makes $\{x, y\}$ a simple pair, whose image is without winding.*

Proof. To simplify the picture we prove the proposition for rotation numbers $\frac{1}{3}$ and $\frac{1}{2}$. The general proof proceeds in the same way. We start by looking at a simple pair $\{x, y\}$ of rotation numbers $\frac{1}{3}$ and $\frac{1}{2}$ for a homeomorphism f with the corresponding invariant graph G given so that the action on it is without any twists, as on the left side of Figures 10 and 11. We now choose a different system of curves (a different graph), in a small neighborhood of G as in Figure 12, which will serve as a new graph for the pair.

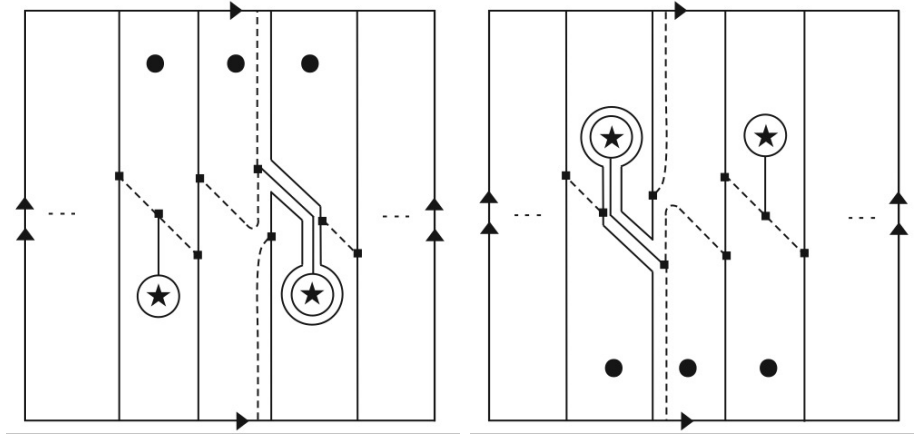


FIGURE 11. The action on a standard graph for a simple pair, for both cases respectively.

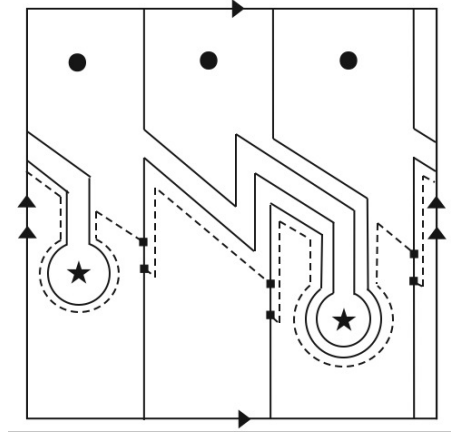


FIGURE 12.

Solid lines are the new vertical loops and dashed lines are the new diagonal segments like in figure 10. The horizontal loop consists of the dashed lines and the long pieces of the solid lines. To move from left to right along the horizontal line, move along a dashed line and turn to the left when meeting a solid line. Continue up along a vertical loop and then along the next dashed line. We add to this graph the peripheral subgraph and the connecting segments and get the graph H as on Figure 13. It is clear that topologically the graph H has the same form as the graph on Figure 10 and that it has an invariant neighborhood.

The reader can check (using the precise knowledge of the image of each edge of the original graph) that the action of f on the graph H

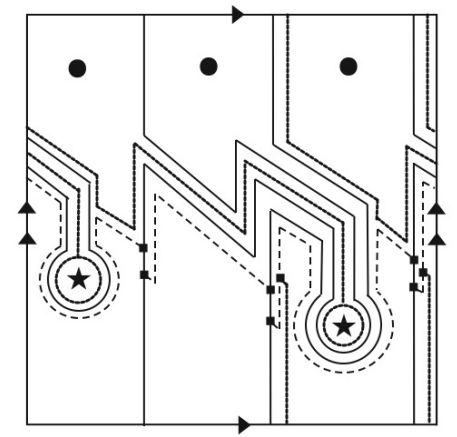


FIGURE 13.

has the properties required from a simple pair. Each vertical loop is mapped onto another vertical loop except for one loop l for which $f(l)$ is equal to a loop m plus a loop around the next periodic point y_p of the shorter orbit. The horizontal loop is mapped onto itself plus a negative Dehn twist along $f(l)$. Consider the image s of the segment which connects the horizontal loop to the periodic point y_{p-1} . When the action has no twist then s moves along the horizontal loop in its positive direction until it meets the original segment connecting to y_p and then it follows along the segment. However in our case s goes first backwards along the horizontal loop than moves in the counterclockwise direction along the boundary of the "rectangle" adjacent to the vertical loop m and finally follows the horizontal loop and the segment to y_p . This means that the action f on the graph H has one positive twist.

We proved that a simple pair for a shear homeomorphism with a given graph and a given action without twists can be given another graph which also describes it as a simple pair and the action on the new graph has one positive twist. This process is reversible. Therefore, by induction, we can add or remove any number of twists using a suitable graph. This implies Proposition 4.2. \square

A neighborhood of the graph can now be given a fibered surface structure, and this fibered surface carries f . Hence, we can apply here the Bestvina-Handel algorithm [2].

For simple pairs, the action in each of the two cases above is easily seen to be tight, as no edge backtracks and for every vertex there are two edges whose images emanate in different directions. The action has no invariant non-trivial forest or nontrivial invariant subgraph and

the graphs have no valence 1 or 2 vertices. This is the definition in [2] for an irreducible map on a graph.

Definition 4.3. Assuming g , the induced map on the graph itself, does not collapse any edges, there is an induced map Dg , the *derivative* of g , defined on

$$\mathcal{L} := \coprod \{(v, e) | v \text{ is a vertex of } G, e \text{ is an oriented edge emanating from } v\}$$

by $Dg(v, a) = (g(v), b)$ where b is the first edge in the edge path $g(a)$ which emanates from $g(v)$.

Definition 4.4. We say two elements (v, a) and (v, b) in \mathcal{L} corresponding to the same vertex v are *equivalent* if they are mapped to the same element under $D(g^n)$ for some natural n . The equivalence classes are called *gates*

The gates in each of the cases above are given by Figure 14, indicated there by small arcs.

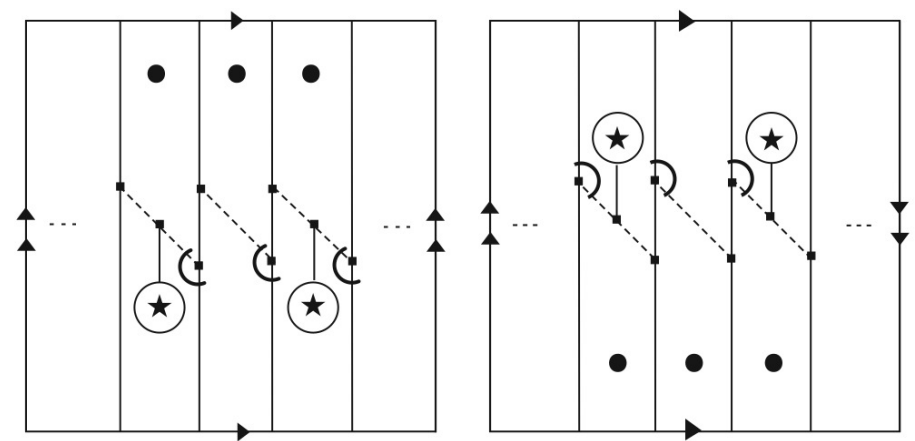


FIGURE 14.

which passes through one of the gates - enters the junction through one arm of the gate and exits through the other. Such an irreducible map is efficient. i.e., this is an end point of the algorithm. Now, since there are edges mapped to an edge path longer than one edge, we arrive at our next theorem.

Theorem 4.5. *A homeomorphism f of the two torus for which a simple pair of periodic orbits exists is isotopic to a pseudo-Anosov homeomorphism relative to this pair of orbits.*

Let f be a shear type homeomorphism of the torus, and fix a lift \tilde{f} of f . Define the *lift rotation number* of a point $x \in \mathbb{T}^2$ to be

$$\rho(x, \tilde{f}) = \lim_{n \rightarrow \infty} \frac{(\tilde{f}^n(\hat{x}) - \hat{x})_1}{n},$$

for any lift \hat{x} of x , when the limit exists, where the subscript 1 denotes the projection to the horizontal axis. Define the *rotation set* $\rho(\tilde{f})$ of \tilde{f} to be the set of accumulation points of

$$\left\{ \frac{(\tilde{f}^n(\hat{x}) - \hat{x})_1}{n} \mid \hat{x} \in \mathbb{R}^2 \text{ and } n \in \mathbb{N} \right\}$$

Then, the above theorem follows from the following much more general theorem by Doeff, see [9].

Theorem 4.6. (Doeff) *Let h be a shear type homeomorphism of \mathbb{T}^2 , and fix a lift \tilde{h} of h . If h has two periodic points x and y with $\rho(x, \tilde{h}) \neq \rho(y, \tilde{h})$ then h is pseudo-Anosov relative to x and y . Furthermore, the closure of the rotation set is a compact interval, and any rational point r in the interior of this interval corresponds to a periodic point $x \in \mathbb{T}^2$ with $\rho(x, \tilde{h}) = r$.*

In particular, Doeff proves existence of two orbits of different rotation numbers implies existence of an orbit for any rotation number between these two. But he does not give any characterization of these orbits. Example 1 shows two different orbits, both with rotation number equal to $1/2$, one of which is pseudo-Anosov, and the other reducible. Thus the rotation number does not give much information about the orbit and in this sense this theorem does not give a satisfactory dynamical understanding of what is happening in regions of coexistence of orbits. In contrast with Doeff's general theorem, we get results for a very specific family of periodic orbits, but for this family we are able to give exactly the orbits forced by others, as we show in section 5.

Now we thicken the edges of the graph to rectangles, which by the Bestvina-Hendel algorithm give a Markov partition for the dynamical system (N, \tilde{f}) . In particular, the rectangles can be glued directly to each other without any junctions. This can be done in a smooth way, endowing N with a compact metric space structure by giving a length and width to each rectangle, consistently, by means of the transition matrix. Each edge of the standard graph for the pair (figure 10) corresponds to one rectangle, except the edge which is mapped to the loop around y_0 . This edge we divide in two (this is necessary to avoid having a rectangle intersecting twice an inverse image of another rectangle). Now we have edges of 7 different types on the graph. The vertical loops

of the graph consist of long edges we denote as A edges, and short edges we call B edges. The loops around the points of the y orbit and vertical segments connecting the loops to the diagonal edges we call C 's and D 's respectively. In rectangles which contain two punctures and therefore two diagonal edges we call the upper ones L edges and the lower ones K edges in the first case, and the lower ones L edges, upper ones K edges, in the second case. The last type of edges are diagonals of once punctured rectangles, these we call M edges.

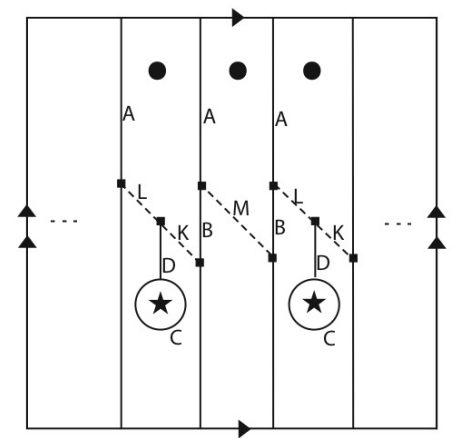


FIGURE 15.

Next, we label the rectangles in order to have explicitly the transition rules:

- For $0 \leq i \leq p_2 - 1$ denote the rectangle corresponding to the D edge connecting the loop around y_i to the diagonal by r_{i+1} . Denote the rectangle corresponding to the C edge which is the loop around y_i by r_{p_2+i+1} .
- For $1 \leq i \leq p_2$, denote the rectangles corresponding to the L and K edges connected to r_i by r_{2p_2+i} and r_{3p_2+i} respectively.
- Denote the rectangle corresponding to the A edge belonging to the vertical line we referred to as m by r_{4p_2+1} and the B edge which is part of the same line m as $r_{4p_2+p_1+1}$.
- For the vertical line $f^i(m)$ denote it's A and B rectangles by r_{4p_2+1+i} and $r_{4p_2+p_1+1+i}$ respectively for all $1 \leq i \leq p_1 - 2$
- For the vertical line $f^{p_1-1}(m)$, denote it's A edge as by $r_{4p_2+p_1}$. There are two rectangles corresponding to the B edge as explained above, denote the lower one by $r_{4p_2+2p_1}$ and the upper one by $r_{4p_2+2p_1+1}$.

- Label the $p_1 - p_2$ remaining rectangles corresponding to the M edges by starting with the first of these to the right of m , and then continuing by the order along the horizontal axis, denoting them by $r_{4p_2+2p_1+2}, \dots, r_{3p_1+3p_2+1}$

Finally, we can look at the diagram in figure 16, showing the set of rectangles and transitions in this Markov partition which we now use.

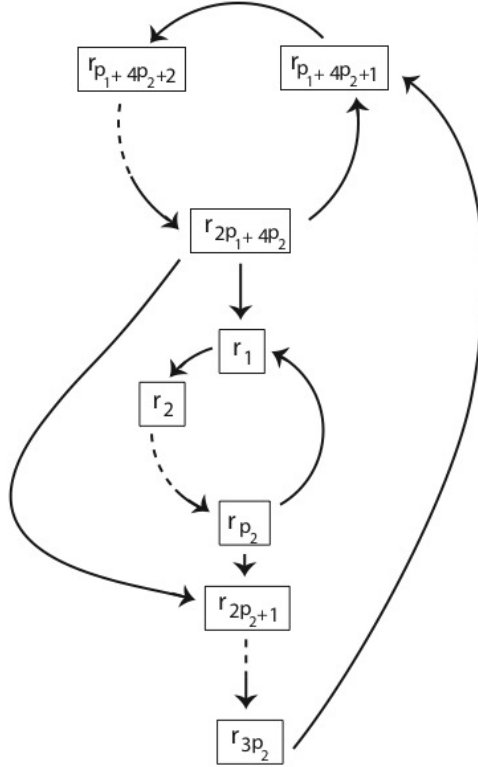


FIGURE 16. Some of the rectangles in the Markov partition, where the arrows denote allowed transitions between them

A periodic symbolic sequence of allowed transitions gives a periodic point in the original dynamical system. Therefore by this diagram we can easily find other periodic orbits on the torus that must exist for f . We will later prove that these orbits are in fact simple, but this will require some more work. Hence, by this diagram we prove only existence of orbits with specified rotation numbers. For every pair (n, m) of natural numbers, $n, m \neq 0$, by starting from $r_{p_1+4p_2+1}$, going n times

around the first loop in the diagram $\{r_{p_1+4p_2+1}, \dots, r_{2p_1+4p_2}\}$, then going $m-1$ times around the second loop $\{r_1, \dots, r_{p_2}\}$ (and skipping it if $m=1$) and then returning through the final sequence $\{r_{2p_2+1}, \dots, r_{3p_2}\}$ to $r_{p_1+4p_2+1}$, we get a periodic symbolic allowed sequence, and so a new periodic orbit we denote $O_{n,m}$. These symbolic sequences are all different and hence so are the periodic orbits. We look at a point $p \in O_{n,m}$ such that p is in the rectangle $r_{p_1+4p_2+1}$. For the first $n \cdot p_1$ iterations of p , corresponding to each time the upper loop in the diagram appears in the symbolic sequence of p , the images are contained in the B edges. The vertical loops are mapped under f retaining the same "horizontal distance" from the periodic points from the x orbit to their left. So, p is mapped a total distance of $n \cdot q_1$ along the horizontal axis under $f^{n \cdot p_1}$.

Similarly, point $f^{np_1}(p)$, which lies in the rectangle r_1 corresponding to D edge, is mapped a distance q_2 along the horizontal axis under each iteration of f^{p_2} , for every occurrence of the second loop in the symbolic sequence of p . This is because the D edges retain their distance from the y orbit points below them. The final sequence in the symbolic representation of p until the return to the first loop also corresponds to the horizontal distance q_1 . These last points of the periodic orbit lie in rectangles corresponding to L edges. So p is mapped a horizontal distance of $nq_1 + mq_2$ under $f^{np_1+mp_2}$. Hence, the new orbit $O_{n,m}$ has rotation number $\frac{nq_1+mq_2}{np_1+mp_2}$.

There is a nice structure on the rationales in the unit interval due to Farey, see [6], which is based on the fact that any such rational can be reached by starting from $0 = \frac{0}{1}$ and $1 = \frac{1}{1}$ and "adding" Farey neighbors $\frac{q}{p}$ and $\frac{r}{s}$ available at each stage by $\frac{q+r}{p+s}$. Thus, any two Farey neighbors span this way all rational numbers between them, so all rationals between $\frac{q_1}{p_1}$ and $\frac{q_2}{p_2}$ are of the form $\frac{nq_1+mq_2}{np_1+mp_2}$. So we found a periodic orbit of any rational number between the two original rotation numbers $\frac{q_1}{p_1}$ and $\frac{q_2}{p_2}$.

This f is a Thurston Nielsen canonical form for the original homeomorphism f and is pseudo Anosov, and so is in fact a condensed representative for f (see [5]). Hence all these periodic orbits belong to different periodic Nielsen types (this is obvious here since they belong to different abelian Nielsen types), and they are all persistent. This yields all these periodic orbits exist for the original f as well. Thus we get theorem 4.6 for our specific case:

Theorem 4.7. *If there exists a simple pair of orbits for a homeomorphism f of the torus of abelian Nielsen types q and p which are Farey*

neighbors, there exists a periodic orbit for f with abelian Nielsen type equal to r for every rational number r between q and p .

5. THE ORDER RELATION

For any simple pair $\frac{\widehat{q_1}}{p_1} \vee \frac{\widehat{q_2}}{p_2}$, The orbit $O_{1,1}$ out of the family of new orbits we constructed above has rotation number equal exactly to $\frac{q_1+q_2}{p_1+p_2}$. This orbit corresponds to the symbolic sequence $r_{p_1+4p_2+1} \rightarrow r_{p_1+4p_2+2} \rightarrow \dots \rightarrow r_{2p_1+4p_2} \rightarrow r_{2p_2+1} \rightarrow \dots \rightarrow r_{3p_2} \rightarrow r_{p_1+4p_2+1}$ as in the diagram in figure 16. So we have a list of rectangles, each containing exactly one periodic point from the new orbit $O_{1,1}$. We denote the point of $O_{1,1}$ that is in a rectangle r_j by o_j . Graphically, assuming the first case map, when we draw the rectangle decomposition corresponding to the standard graph as in figure 10 we get Figure 17.

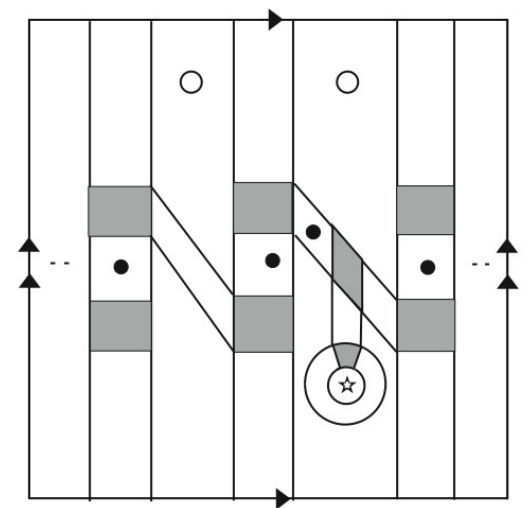


FIGURE 17. The intermediate orbit denoted by black circles. The gray areas are junction, which can be deleted, and the rectangles can be glued directly to one another.

We will now show that for any simple pair $\frac{\widehat{q_1}}{p_1} \vee \frac{\widehat{q_2}}{p_2}$ the orbit $O_{1,1}$ is a simple orbit, and forms a simple pair with each periodic orbit of the pair, that is with $\frac{\widehat{q_1}}{p_1}$ and $\frac{\widehat{q_2}}{p_2}$. For the first assertion, we define a family of vertical loops as follows: we choose a vertical loop that crosses both rectangles corresponding to the m line and passes to the right of the periodic point $o_{p_1+4p_2+1}$. Denote this loop by A . It is shown graphically in figure 18. All its images under f till the p_1 st iteration are exactly of the same form, as the rectangles are simply mapped to

the right without changing their forms. Its p_1 st image is the first time it returns to the same rectangles, and is determined by the images of the corresponding vertical edges of the graph. These images are shown in figure 11. We use the fact f preserves orientation to determine the relation between the image of the curve and the points of $O_{1,1}$. We denote this image by B . It is shown in figure 18.

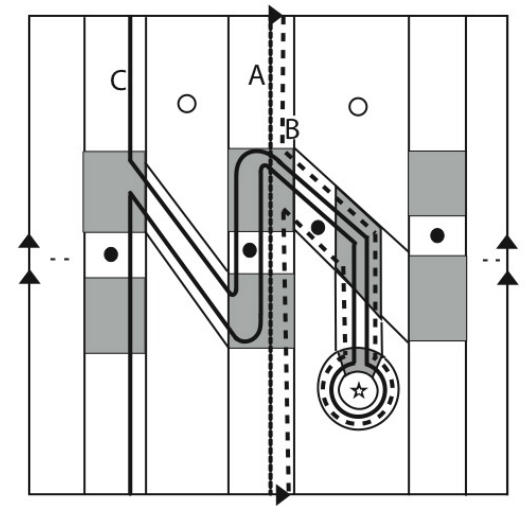


FIGURE 18. The intermediate orbit with the family of vertical loops

Out of similar considerations, knowing the rectangles containing B in the original picture (Figures 10 and 11) the rectangle adjacent to $f^{p_1-1}(m)$ on the left contains a point of the y -orbit and therefore contains a rectangle of type L of Markov partition. This rectangle contains the point o_{3p_2} of the new orbit. Line A lies to the right of m and of $o_{p_1+4p_2+1}$ therefore $f^{p_1-1}(A)$ lies to the right of o_{3p_2} and to the right of $o_{2p_1+4p_2}$. It follows that the line $B = f^{p_1}(A)$ lies to the right of $o_{p_1+4p_2+1}$ and to the right of o_{2p_2+1} , as shown on Figure 18. Also B can be isotoped to the right of A relative to the points of the new periodic orbit. Next $p_2 - 1$ iterations of f translate A and B and whole rectangle adjacent to m on the right to the right. We arrive at the rectangle adjacent to l on the left containing point o_{3p_2} of the new orbit. The point $o_{2p_1+4p_2}$ lies in a rectangle on the line l . The loop $f^{p_2-1}(B)$ lies to the right of o_{3p_2} and to the left of $o_{2p_1+4p_2}$ therefore the loop $C = f^{p_2}(B)$ lies to the right of $o_{p_1+4p_2+1}$ and to the left of o_{2p_2+1} , as shown on Figure 18. Also p_2 iterations of f take line m to a distance $p_2q_1 = p_1q_2 - 1$ rectangles to the right, which means one rectangle to the left of line m . Since A and B are to the right of the point $o_{p_1+4p_2+1}$

in line m and since this point moves to the leftmost point in the new periodic orbit shown on Figure 18, loop C must be to the right of it, as in Figure 18. The point o_{2p_1+1} may be above or below the loop C but this does not change the discussion below.

Note that if we disregard the orbits x and y of the original pair we can isotope C to A relative the points of the new orbit. This shows that the new orbit is a simple periodic orbit of length $p_1 + p_2$, by Lemma 3.3. Now we fill in the x orbit (the longer orbit) and consider a torus punctured at the y orbit and the new orbit together. We have the family of vertical loops $f^i(A)$ and the action on it is exactly as in the condition for a simple pair as the loop C can be isotoped to A plus a loop around y_0 . We choose a horizontal loop as the loop D on Figure 19. Then its image D' is as shown on Figure 19. The image has the required properties. The orbit y together with the new orbit form a simple pair for the homeomorphism f .

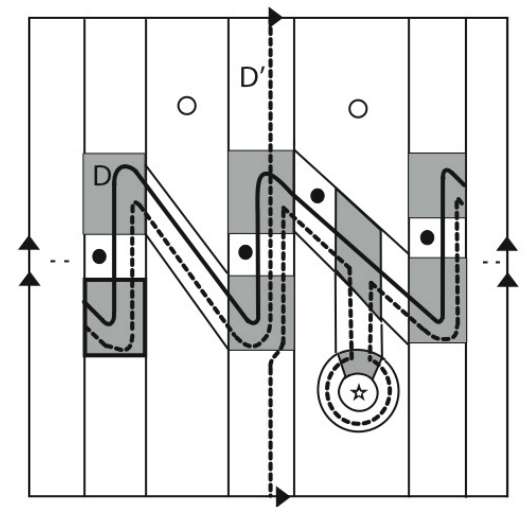


FIGURE 19.

Next we fill in the y orbit and leave punctures at the x orbit and the new orbit. We choose the initial vertical loop A differently, as in Figure 20. This loop A is one rectangle to the right of m plus a loop on the left. After $k = p_2 - 1$ iterations of f it will move to line l which is q_1 rectangles to the left of m . Indeed it will move to $q_1(p_2 - 1) + 1 = p_1q_2 - q_1$ rectangles to the right of m which means q_1 rectangles to the left. The loop $f^k(A)$ looks like the loop A and lies to the left of the point r_{3p_2} and to the left of the point $o_{2p_1+4p_2}$. Next iteration of f takes it to a curve which looks like $f(l)$ but lies to the left of $o_{p_1+4p_2+1}$ and to the left of o_{2p_2+1} . Since we filled the point y_0 we

can isotop this loop to a vertical loop near m , which passes to the left of $o_{p_1+4P_2+1}$. Subsequent iterations translate it to the right and $f^{p_1}(A)$ is equal to curve B on Figure 20

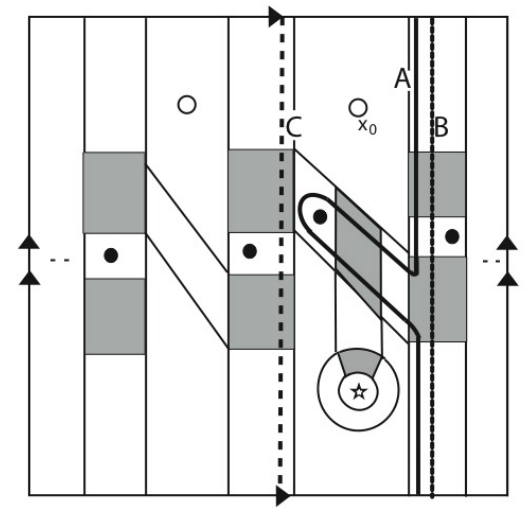


FIGURE 20.

Next $p_2 - 1$ iterations will take B to the loop near l which lies to the left of $o_{2p_1+4p_2}$. Next iteration of f takes this loop to a loop similar to $f(l)$, but lies to the left of o_{2p_2+1} . Since the points of y -orbit are filled we can isotop it to the loop C on Figure 20. It can be further isotoped, relative to the x -orbit and the new orbit, to the loop A plus a small loop around x_0 to the left of A . If we choose the same horizontal loop as in the previous case, with the same image as before, we get the required action of f for a simple pair consisting of the x -orbit and the new orbit.

Now we can continue by the same analysis for each of these two simple pairs, finding their Farey intermediate to be a simple orbit as well that forms a simple pair with each of them, and so on. Thus we have proven our main result, Theorem 1.1.

6. GLOBAL ANALYSIS OF THE KICKED ACCELERATED PARTICLE SYSTEM

The physical system called the kicked accelerated particle consists of particles that do not interact with one another. They are subject to gravitation and so fall downwards, and are kicked by an electromagnetic field, i.e., the electro magnetic field is turned on for a very short time once in a fixed time interval. This electromagnetic field is a

sine function of the height of the particle, hence the particles are kicked upwards or downwards by different amounts, depending on their position at the time of a kick. For a short review of the results for this system see [8]. Experiments of this system were conducted by the Oxford group, see [13], and the system was found to show a phenomena that is now called "quantum accelerator modes": as opposed to the natural expectation that particles fall with more or less the gravitational acceleration, it was found that a finite fraction of the particles fall with constant nonzero acceleration relative to gravity, as can be seen in Figure 21

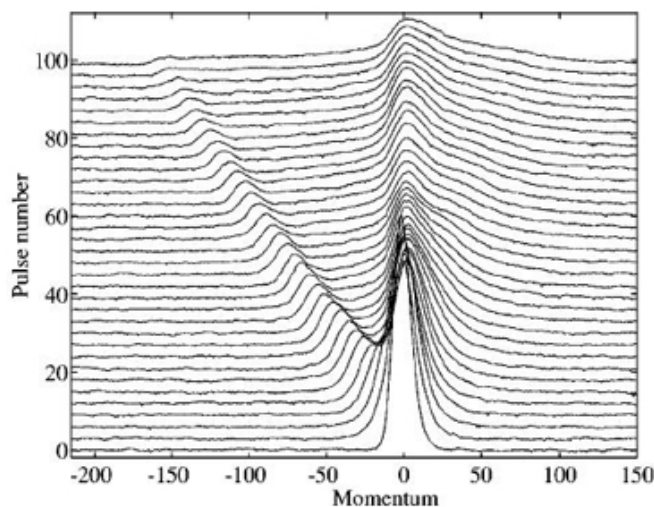


FIGURE 21. Accelerator modes

Experimental Data (taken from Oberthaler, Godun, d'Arcy, Summy and Burnett, see [13]) showing the number of atoms with specified momentum relative to the free falling frame as the system develops in time (the numbers on the y axis represents time by the number of kicks, while the z coordinate is proportional to the number of atoms)

This is a truly quantum phenomenon having no counterpart in the classical dynamics. A theoretical explanation for this phenomenon was given by Fishman, Guanieri and Rebuzzini in [10], and it establishes a correspondence between accelerator modes of the physical system, and periodic orbits of the classical map

$$(1) \quad f : \begin{pmatrix} J \\ \theta \end{pmatrix} \mapsto \begin{pmatrix} J + \tilde{k} \sin(\theta + J) + \Omega \\ \theta + J \end{pmatrix} \mod 2\pi$$

Where the J coordinate corresponds to the particles momentum, and θ to its coordinate. This map is of shear type, and the acceleration for a periodic orbit with rotation number $\frac{q}{p}$ is given by

$$(2) \quad \alpha = \frac{2\pi q}{p} - \Omega$$

Hence, by analyzing the structure of existence of periodic orbits for the classical map above, we would be able to find which modes should be expected for which values of the parameters k and Ω . We remark that actual experimental observation also requires stability of the periodic orbits. It is important to stress here that since these parameters correspond to the kick strength and the time interval between kicks they can be controlled in the experiments as we wish, so results obtained for this system can be tested experimentally. When one plots the numerical results describing which periods exist for different values of k and Ω one gets an extremely complicated figure, see figure 22.

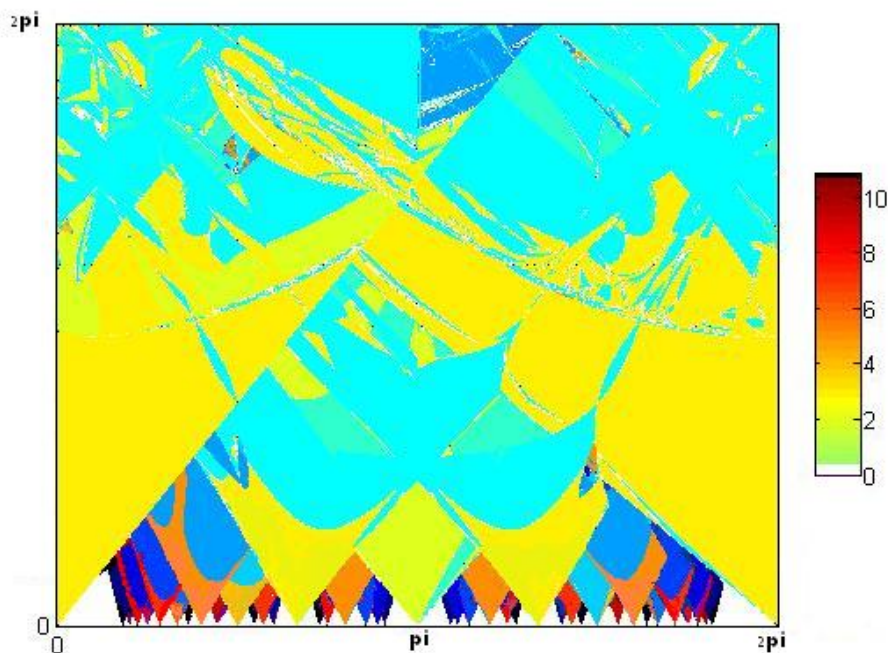


FIGURE 22. Tongues of periodic orbits

An exact mathematical analysis of this system is extremely complicated. Perturbative methods have been used in [10] to analyze the existence of these "tongues" of periodic orbits in the region where $k \rightarrow 0$, as well as giving estimates on their widths.

Look at the map f given by (1) in regions where Ω is equal $\frac{q}{p}2\pi$ for some rational number $\frac{q}{p}$ in the unit interval, and small k . For a small enough k it can be seen both from the numerical results shown graphically in figure 22 and from perturbative arguments that in the above region a periodic orbit with period p exists.

For small k the periodic points of this orbit must be pretty much equally spaced along the J axis, and we can choose (for k small enough) a family of vertical loops that are equally spaced at distance exactly Ω apart, and each is at distance at least, say, $3k$ from any of the periodic points.

The image of a loop parameterized by $\Gamma_1(\theta) = \begin{pmatrix} J_0 \\ \theta \end{pmatrix}$ is given by $\begin{pmatrix} J_0 + k\sin(J_0 + \theta) + \Omega \\ J_0 + \theta \end{pmatrix} = \begin{pmatrix} J_0 + k\sin(\theta') + \Omega \\ \theta' \end{pmatrix}$ and so is very close (for small k) to another loop of the chosen family. It follows that there exists a map \tilde{f} isotopic to f rel the orbit which keeps this family of curves invariant, and so, by lemma 3.3, all the periodic orbits seen in the tips of the tongues in Figure 22 are simple orbits.

Note the rotation number of each of these orbits is equal exactly to the value of Ω in the tip of the tongue ($k = 0$) as for very small k the J coordinate increases by an almost fixed value, close as we wish to Ω . And, by equation (2) the rotation number $\frac{q}{p}$ is related to the acceleration of the corresponding acceleration mode by

$$\alpha = \frac{q}{p}2\pi - \Omega$$

So the topological meaningful numbers here are in fact also the ones with physical significance. While Ω changes through the region in which this periodic orbit exists, $\frac{q}{p}$ is of course a topological invariant and therefore fixed. Hence the acceleration vanishes on the line with fixed Ω in the middle of each tongue, and changes signs when one crosses this line. This was measured experimentally in [11].

For any other point higher in the tongue which we can reach by an isotopy along which the periodic orbit exists, we also have the orbit is a simple orbit. We will assume, as is very natural and was checked numerically for many cases, that the orbits remain simple throughout the region of each tongue.

In some of the cases for which we drew a portrait of the phase space, we found that the fact the homeomorphism is isotopic to one which is

reducible rel the periodic orbit is realized by the physical map itself, as seen in Figure 23.

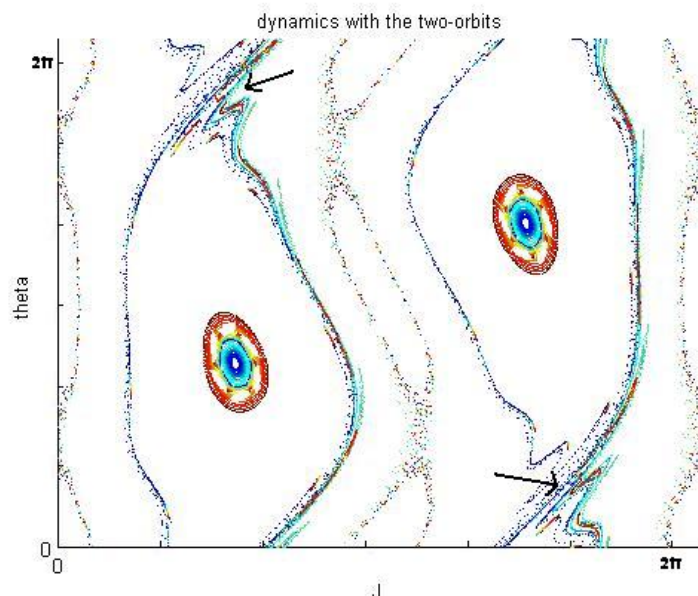


FIGURE 23. Phase portrait for a two-orbit

Drawn for $k = \frac{1}{15}2\pi$ and $\Omega = \pi$, the two-orbit which is clearly seen is a stable orbit with two stable neighborhoods drawn. There is another two-orbit present, at which the arrows point, and it is the stable and unstable manifolds for this unstable orbit which divide the phase space into non intersecting regions which do not mix.

Here the phase space is truly divided into pieces. Each of the annuli in this decomposition is mapped to another, and returns to itself with one twist after p iterations of f . Therefore every periodic orbit must have a period which is a multiple of p . On the other hand, when an annulus is mapped to itself with one twist under an area preserving map (here under f^p), every rotation number in the unit interval exists for it (here we mean the standard annulus rotation number measuring the rotations around the annulus), and so every period exists, as for every rational number $\frac{n}{m}$ there is a periodic point of order m which rotates n times around the annulus before it returns to itself. This yields that for such a point in the parameter space, exactly all periods that are multiples of p exist. It is our belief that this situation is typical for the center of each tongue, that is for $\Omega = 2\pi\frac{q}{p}$. At other points, namely in all point we have numerically checked outside the center of

the tongue, orbits of coprime lengths may exist simultaneously. We believe that the coexisting orbits whose rotation numbers are Farey neighbors form a simple pair together, as in the example on Figure 24, which shows a simple pair of orbits with rotation numbers $1/3$ and $1/2$ found in the physical system.

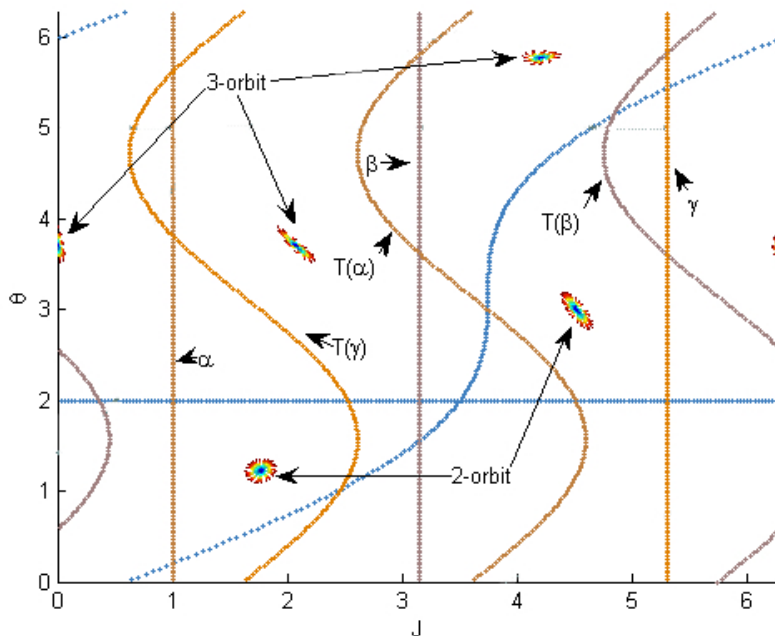


FIGURE 24. A pair of coexisting orbits in the physical system
 Drawn with a collection of curves on the torus and their images,
 which show this is a simple pair.

This coexistence happens at a point in Figure 22 for which two tongues intersect. We assume that the same orbit persists throughout the tongue, and therefore we have at such a point two coexisting simple orbits. We believe that in all points of intersecting tongues coming from $k = 0$ and $\Omega_1 = \frac{q_1}{p_1}$, $\Omega_2 = \frac{q_2}{p_2}$ which are Farey neighbors, $p_1 > p_2$, the coexisting orbits form a simple pair.

Theorem 4.7 therefore implies that there are infinitely many periodic orbits for the parameters at a region of intersection of two such tongues, with rotation numbers equal to all rational numbers between the ones of these two tongues. If we assume all these simple orbits present also come from tongues, this yields that each rational tongue between $\frac{q_1}{p_1}$ and $\frac{q_2}{p_2}$ intersects each of these two tongues lower (along the k axis) than they intersect each other. In other words, following a path from a tip of

a tongue upwards in the tongue, if it intersects a Farey neighbor tongue we know it intersects earlier all tongues of rational numbers between them. This determines the global structure appearing in Figure 22 of all accelerator modes in the physical system, as Sharkovskii's theorem determines it for one dimensional systems.

REFERENCES

- [1] R. L. Adler 1998 Symbolic dynamics and Markov partitions *Bulletin of the AMS* **35** N1 1-56
- [2] M. Bestvina and M. Handel 1992 Train-tracks for surface homeomorphisms *Topology* **34** 109-140
- [3] P. Boyland 1988 An analog of Sharkovskii's theorem for twist maps. *Hamiltonian Dynamical systems* 119-133. Contemporary Mathematics 81, American Mathematical Society.
- [4] P. Boyland 1994 Topological methods in surface dynamics *Topology and its applications* **58** 223-298
- [5] P. Boyland 1999 Isotopy stability for dynamics on surfaces, Geometry and topology in dynamics *Contemp. Math.* **246** 17-45
- [6] G. H. Hardy and E. M. Wright 1979 *An introduction to the theory of numbers*. Clarendon Press, Oxford.
- [7] A.J. Casson, S.A. Bleiler 1988 *Automorphisms of surfaces after Nielsen and Thurston*
- [8] M.B. d'Arcy, G.S. Summy, S. Fishman and I. Guarneri 2004 Novel Quantum Chaotic Dynamics in Cold Atoms, *Physica Scripta* **69**, C25-31
- [9] E. Doeff 1997 Rotation measures for homeomorphisms of the torus homotopic to a Dehn twist *Ergod. Theor. Dynam. Syst.* **17** 1-17
- [10] S. Fishman, I. Guarneri and L. Rebuzzini 2003 *J. Stat. Phys.* **110** 911; S. Fishman, I. Guarneri and L. Rebuzzini 2002 *Phys. Rev. Lett.* **89** 84101-1-4; I. Guarneri, L. Rebuzzini and S. Fishman, Arnol'd Tongues and Quantum Accelerator Modes, submitted for publication in Nonlinearity, (quant-ph/0512086)
- [11] Z-Y. Ma, M.B. d'Arcy and S. Gardiner 2004 *Phys. Rev. Lett.* **93** 164101-1-4
- [12] T. Matsuoka 1986 Braids of periodic points and a 2-dimensional analogue of Sharkovskii's ordering, *World Sci. Adv. Ser. in Dynamical Systems* **1** 5872
- [13] M.K. Oberthaler, R.M. Godun, M.B. d'Arcy, G.S. Summy, and K. Burnett 1999 *Phys. Rev. Lett.* **83** 4447-4451

Tali Pinski
Department of Mathematics
The Technion
32000 Haifa, Israel
e-mail: otali@tx.technion.ac.il

Bronislaw Wajnryb
Institute of Mathematics of the Polish Academy of Science
ul. Sniadeckich 8
00-956 Warszawa, Poland
e-mail: bronekww@wp.pl